This is a repository copy of *3D Steganalysis Using LaplacianSmoothing at Various Levels*.

White Rose Research Online URL for this paper:
https://eprints.whiterose.ac.uk/id/eprint/147011/

Version: Accepted Version

3D Steganalysis Using Laplacian Smoothing at Various Levels

Zhenyu Li[1], Fenlin Liu[2][*], and Adrian G. Bors[1]

[1] University of York, Department of Computer Science, York YO10 5GH, UK
[2] Zhengzhou Science and Technology Institute, Zhengzhou 450000, China

Abstract. 3D objects are becoming ubiquitous while being used by many mobile and social network applications. Meanwhile, such objects are also becoming a channel being used for covert communication. Steganalysis aims to identify when information is transferred in such ways. This research study analyses the influence of the 3D object smoothing, which is an essential step before extracting the features used for 3D steganalysis. During the experimental results, the efficiency when employing various degrees of 3D smoothing, is assessed in the context of steganalysis.

Keywords: 3D steganalysis, Laplacian smoothing, local feature, information hiding

1 Introduction

3D objects are used in many applications, including graphics, virtual reality, visualization and so on. In order to be used by many applications, 3D objects are increasingly transferred shared between users through clouds or mobile media. When compared to the steganalysis research on other media, such as images [15, 20, 1, 30, 17], video[24, 29] and audio signals [18, 19], the steganalysis for 3D objects is much less developed, resulting in a lower likelihood of identifying the information hidden in 3D objects. Many 3D information hiding algorithms have already been proposed [5, 3, 28, 16, 2, 8, 12]. Nevertheless, secret information transferred through 3D objects could pose a threat to the public security, when used by terrorists or criminals.

So far there are much fewer steganalytic approaches for 3D objects than for images and video signals. The first steganalytic algorithm for 3D meshes was proposed in [26]. This 3D steganalytic algorithm is based on the features of 3D meshes and by using machine learning, for distinguishing stego-objects from cover-objects. During 3D steganalysis, both cover- and stego-objects are smoothed using one Laplacian smoothing iteration. Then, the geometric features such as the vertex location and norm in Cartesian and Laplacian coordinate systems [25], the dihedral angle of edges and face normals, are extracted from the

---

[*] The corresponding author, e-mail address: liufenlin@sina.vip.com

original mesh and the smoothed one. It calculates the absolute differences between the features from the original mesh and those from the smoothed mesh. The feature vectors used for steganalysis are the four statistical moments of the logarithm of the absolute differences between the object and its smoothed counterpart. Meanwhile, the histograms of the differences between the features corresponding to the original objects and their smoothed counterparts are formed and used for extracting the steganalytic features. Finally, the steganalytic approach uses quadratic discriminate analysis to train the classifiers for separating the stego-objects, produced by several steganographic algorithms from their corresponding cover-objects.

More recently, Yang *et al.* [27, 28] proposed a new steganalytic algorithm, specifically designed for the robust 3D watermarking algorithm, MRS, proposed in [5]. During steganalysis, the number of bins, K, used in the watermarking algorithm is estimated using exhaustive search. For each K, the steganalytic algorithm classifies the bins into two clusters using a standard clustering algorithm fitting the data with a mixture of two Gaussian distributions. The estimate of K corresponds to that which maximizes the Bhattacharyya distance between the two clusters. Then it uses a normality test to decide if the bins of the mesh can be modeled by a single Gaussian, in which case the mesh would not contain any hidden information. Otherwise, the distribution is bimodal and consequently the mesh is watermarked. The limitation of this algorithm is that it is only effective for the information embedded by the MRS algorithm and would not be useful when the mesh is embedded by other information hiding algorithms than MRS.

Li and Bors proposed the 52-dimensional Local Feature Set (LFS52) in [13], which simplified the 208-dimensional feature set YANG208 proposed in [26] and included some new geometric feature for steganalysis, such as the vertex normal, the curvature ratio and the Gaussian curvature. In addition to LFS52, other geometric features extracted from the mesh, such as the edge length and vertex position represented in the spherical coordinate system, form the 76-dimensional feature set for 3D steganalysis in [14]. Kim *et al.* [9] extended the approach from [13], and proposed to use some additional features such as the edge normal, mean curvature and total curvature as supplement to LFS52 and formed LFS64 for 3D steganalysis.

In this research study we use various levels of high-pass filtering, before extracting various sets of features for image steganalysis. The existing 3D steganalysis framework based on the local feature set is briefly summarized in Section 2. The main idea of the proposed method is introduced in Section 3. The experimental results and the conclusion are given in Sections 4 and 5, respectively.

2   3D steganalysis framework based on local feature set

In this section, we provide a brief introduction of the 3D steganalysis framework based on the local feature set, LFS76, proposed in [14], as illustrated in Figure 1.
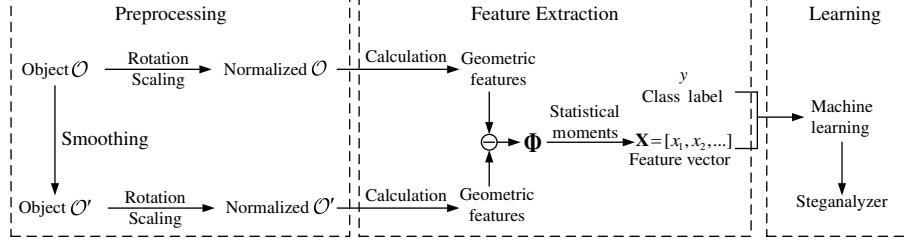
Fig. 1. The 3D steganalysis framework based on learning from statistics of the 3D features and classification by means of machine learning methods.

The 3D steganalyzer is trained through the following processing stages: preprocessing, feature extraction and supervised learning. During the preprocessing step, a smoothed version of the given original mesh, $\mathcal{O}'$, is obtained by applying one iteration of Laplacian smoothing on the original mesh, $\mathcal{O}$. Then, the original mesh and its smoothed version are both normalized by using rotation and scaling. The idea of 3D object smoothing was inspired by the calibration technique used in image steganalysis [6, 10]. It is based on the assumption that the difference between a mesh and its smoothed version is larger for a stego mesh than for a cover mesh. In most 3D watermarking algorithms, the changes produced to the stego-object can be associated to noise-like changes. Consequently, when smoothing a cover mesh, the resulting modifications will be smaller than those obtained when smoothing its corresponding stego mesh.

During the feature extraction, 19 geometric features, characterizing the local geometry of 3D shapes, are extracted from the original mesh, $\mathcal{O}$, and its smoothed version, $\mathcal{O}'$. These geometric features define the vertex coordinates and norms in the Cartesian and Laplacian coordinate systems, the face normal, the dihedral angle, the vertex normal, the Gaussian curvature, the curvature ratio, the vertex coordinates and edge length in the spherical coordinate system. The differences between the mentioned geometric features from $\mathcal{O}$ and those from $\mathcal{O}'$ are denoted as the vector $\boldsymbol{\Phi} = \{\phi_t | t = 1, 2, .., 19\}$. Afterwards, the first four statistical moments, representing the mean, variance, skewness and kurtosis, of the logarithm of the differences, $\{\lg(\phi_t) | \phi_t \in \boldsymbol{\Phi}\}$, are considered as the steganalytic features, resulting in the 76-dimensional local feature set, LFS76, representing the input into the steganalyzer.

The steganalyzers are trained using the Fisher Linear Discriminant (FLD) ensemble [11] which is broadly used for image steganalysis as well [15, 20, 21]. The FLD ensemble includes a number of base learners trained uniformly on the randomly selected feature subsets extracted from the whole training data. The FLD ensemble uses the majority voting in order to combine the results of all base learners, achieving a much higher accuracy than any of the individual base learners.

3   Assessing the effects of 3D object smoothing, as a preprocessing stage for steganalysis

The steganalytic approaches for 3D objects have been influenced by the technology of image steganalysis to a large extent. In order to capture the various types of dependencies among the neighboring pixels, many studies in the image steganalysis, such as [7, 20], propose to apply different high-pass filters in order to remove various levels of low level of detail. The removal of low level detail is an essential processing stage, which is followed by the robust extraction of steganalytic features. This approach is inspired from image smoothing, commonly used as a pre-processing step for image steganalysis. In the following, we assess the influence, when employing various degrees of smoothing, on the 3D steganalysis.

Let us assume that we have a given mesh $\mathcal{O} = \{V, F, E\}$, containing the vertex set $V = \{v(i) | i = 1, 2, \ldots, |V|\}$, where $|V|$ represents the number of vertices in the object $\mathcal{O}$, its face set F, and its edge set E, respectively. We define the 1-ring neighbourhood $\mathcal{N}(v(i))$ of a vertex $v(i)$ as $\{v(j) \in \mathcal{N}(v(i)) | e(i, j) \in E\}$, where $e(i, j)$ is the edge connecting vertices $v(i)$ and $v(j)$.

We consider Laplacian smoothing for the given object $\mathcal{O}$, resulting in its smoothed version $\hat{\mathcal{O}}^{(\lambda, k)}$ after k iterations of smoothing with the scale factor λ. When one iteration of Laplacian smoothing is applied to the 3D object $\mathcal{O}$, it updates the vertex v_i into v'_i in $\hat{\mathcal{O}}$ as follows, [22]:

$$v'_i \leftarrow v_i + \frac{\lambda}{\sum_{v_j \in \mathcal{N}(v_i)} w_{ij}} \sum_{v_j \in \mathcal{N}(v_i)} w_{ij}(v_j - v_i), \tag{1}$$

where λ is the scale factor and w_{ij} are the weights defined as:

$$w_{ij} = \begin{cases} 1 & \text{if } v_j \in \mathcal{N}(v_i) \\ 0 & \text{otherwise} \end{cases} \tag{2}$$

.

In equation (1) we use a 1-ring neighbourhood for smoothing. So after two iterations of smoothing, the information provided by a 2-ring neighbourhood would be considered for smoothing. It is obvious that a larger number of iterations of the smoothing leads to considering the influence of the vertices from a larger neighbourhood of the given vertex, during the smoothing, resulting in different levels of smoothing as well. However, adjusting the value of λ, we can control the level of the smoothing, without actually enlarging the neighbourhood of the vertex. The influence of choosing different values of λ and numbers of iterations k is investigated in the Section 4.

After applying different numbers of iterations of the Laplacian smoothing with various scale factors to the given $\mathcal{O}$, we obtain a set of original and smoothed object pairs $\{< \mathcal{O}, \hat{\mathcal{O}}^{(\lambda, k)} > | \lambda \in \mathbb{R}, k \in \mathbb{N}\}$. The 19 geometric features, $\{\phi_t(i, j) | t = 1, ..., 19\}$, proposed in [14], are extracted from every original and smoothed object pair, $< \mathcal{O}, \hat{\mathcal{O}}^{(\lambda, k)} >$. Then, we follow the same approach as in [14] to form the steganalytic features. Considering the first four statistical moments, representing the mean, variance, skewness and kurtosis, of the logarithm of the statistics,

$\{\lg{(\phi_t)}|\phi_t \in \mathbf{\Phi}\}$, we have the 76-dimensional local feature set for each original and smoothed object pair. Eventually, we combine all the feature sets, obtained from multiple original and smoothed object pairs, into an enlarged feature set to be used for steganalysis.

4 Experimental results

In the following we provide the results for the proposed 3D steganalytic approach on 354 cover 3D objects from the Princeton Mesh Segmentation project database [4]. This database contains a large variety of shapes, representing the human body under a variety of postures, statues, animals, toys, tools and so on. Some objects used in the experiment are shown in Figure 2.
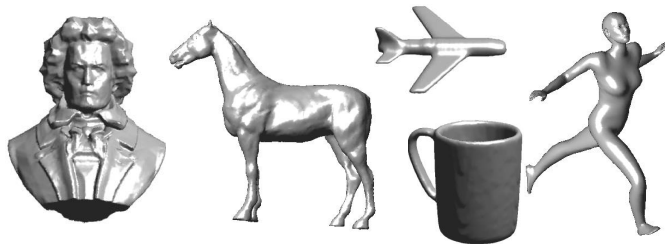

Fig. 2. 3D objects used in the steganalytic tests.

We consider identifying the 3D stego-meshes produced by using four different embedding algorithms: the Multi-Layer Steganography (MLS) provided in [3], a blind robust watermarking algorithms based on modifying the Mean of the distribution of the vertices' Radial distances in the Spherical coordinate system, denoted as MRS, from [5], the Steganalysis-Resistant Watermarking (SRW) method proposed in [28] and the Wavelet-based High Capacity (WHC) watermarking method proposed in [23]. When using the MLS method from [3], we set the number of layers to 10, and consider the number of intervals as 10000. For the MRS watermarking methods from [5], we consider $\alpha = 0.04$ for the watermark strength, while fixing the incremental step size to 0.001 and the message payload as 64 bits. During the generation of the stego-meshes using the SRW method from [28], we set the parameter $K = 128$ which determines the number of bins in the histogram of the radial distance coordinates for all vertices. According to [28], the upper bound of the embedding capacity is $\lfloor (K-2)/2 \rfloor$ bits. The parameter that controls the watermarking robustness of SRW is n_{thr}, which is set at 20. If the smallest number of elements in the bins from the objects is less than 20, we would choose the smallest nonzero number of elements in the bins as n_{thr}. With regards to the parameters involved in WHC, we set the control parameter $\epsilon_{hc} = 100$ and other parameters are all identical to the values from [23]. The embedded information is a pseudorandom bit stream which simulates the secret messages or watermarks hidden by the steganographier.
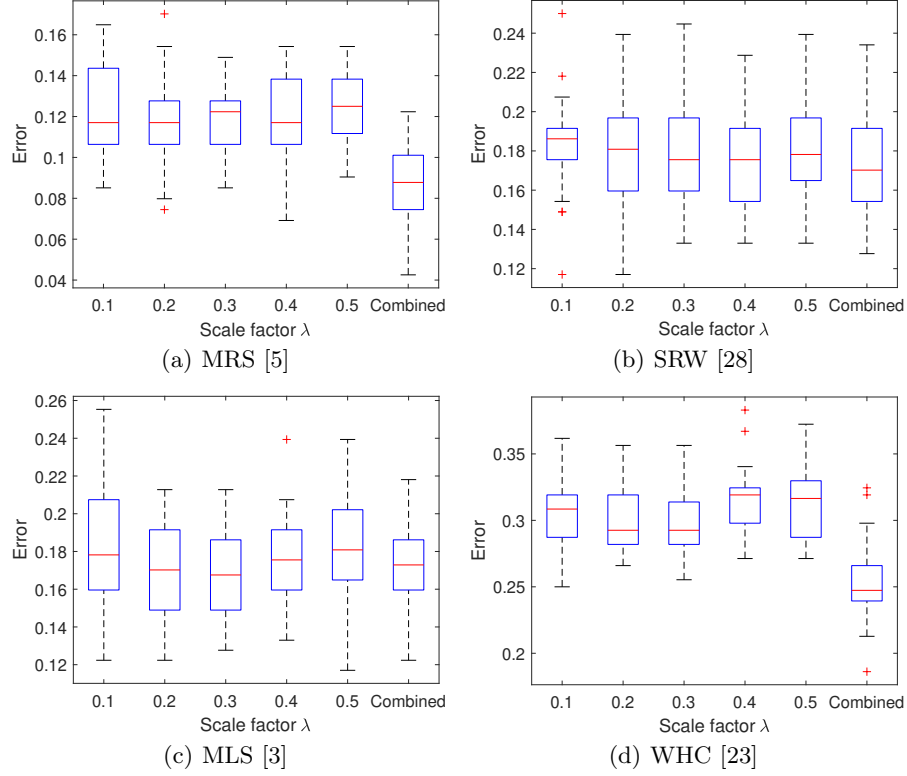
Fig. 3. Box plots showing the confidence intervals for the detection errors for the three 3D information embedding algorithms when the scale factor, λ, varies during the feature extraction when considering the LFS76 feature set. The "Combined" represents the results of the combined feature set with $\lambda \in \{0.1, 0.2, 0.3, 0.4, 0.5\}$.

The steganalyzers are trained using the FLD ensemble, as in [14]. For each steganalyzer, we split the 354 pairs of cover-mesh and stego-mesh into 260 pairs for training and 94 pairs for testing, repeating independently the experiments for 30 times. The steganalysis results are assessed by calculating the median value of the detection errors which are the sums of false negatives (missed detections) and false positives (false alarms) from all 30 trials. Laplacian smoothing is used as a pre-processing stage on 3D objects, before the feature extraction, as shown in left part of the diagram from Figure 1. In the following we analyse the effects of various parameters involved in the 3D objects' smoothing.

4.1 Studying the effect of smoothing when varying the scale factor λ

In order to investigate the influence of the scale factor, λ, on the efficiency of the steganalytic features, we vary the scale factor $\lambda \in \{0.1, 0.2, 0.3, 0.4, 0.5\}$ which

is being used for a single iteration of Laplacian smoothing, according to equation (1), during the preprocessing stage of the extraction of the LFS76 feature set. The LFS76 feature set is extracted from the cover-meshes and the corresponding stego-meshes when embedded with information by four 3D embedding algorithms, MRS [5], SRW [28], MLS [3] and WHC [23]. We also adopt the strategy proposed in this paper by combining the LFS76 feature sets extracted when considering various levels of object smoothing by varying λ.

We use the feature sets obtained as mentioned above to train the steganalyzers for four embedding algorithms respectively. The box plots of the testing results are provided in Figure 3. It can be observed from Figure 3, that the steganalysis results do not change much when varying the smoothing scale factor λ, in the case when embedding information into 3D objects by the MRS and SRW algorithms. When the scale factor $\lambda = 0.3$, the steganalysis results for the 3D objects embedded by the MLS and WHC algorithms are slightly better than the results obtained when $\lambda \in \{0.1, 0.2, 0.4, 0.5\}$. Nevertheless, when combining the objects resulting from the smoothing by using all five different scales $\lambda \in \{0.1, 0.2, 0.3, 0.4, 0.5\}$, we achieve a better performance than any of the individual feature sets in the case of MRS and WHC, as it can be observed from the results presented in Figures 3(a) and (d).

4.2 Varying the number of iterations for Laplacian smoothing

In the following, we evaluate the efficiency of the steganalysis, when varying the number of iterations for the Laplacian smoothing. During the Laplacian smoothing, the scaling factor λ is fixed at 0.3, which provides a stable performance according to the results shown in Figure 3. We first extract the LFS76 feature set based on the Laplacian smoothing when varying the number of iterations as $k \in \{1, 2, 3, 4, 5\}$. Then, according to the same procedure as that used in the previous section, we combine the 5 feature sets obtained into a whole feature set with the dimensionality of $76 \times 5 = 380$.

The performance of the various feature sets mentioned above are tested by the detecting the embedding changes produced by four embedding algorithms, MRS [5], SRW [28], MLS [3] and WHC [23]. The detection results are provided in Figure 4. It is shown in Figures 4(a), (b) and (d) that the combined feature set achieves better performance than any of the individual feature sets (using only a certain number of iterations) in the case of MRS and SRW. However, the combined feature set does not improve the detection accuracy compared to the best individual LFS76 feature set $(k = 1)$ when the information are embedded by MLS algorithms, as shown in Figure 4(c). It also can be seen from Figure 4(c) that when the number of iterations of the Laplacian smoothing increases, the detection error for the MLS increases as well. This is because by increasing the level of smoothing too much, we may remove essential features produced by the MLS steganographic algorithm or even 3D object features. In such situations, excessive smoothing would affect negatively the 3D steganalysis.

The experimental results provided in Figures 3 and 4 indicate the effects when varying the smoothing scaling parameter and the number of iterations,
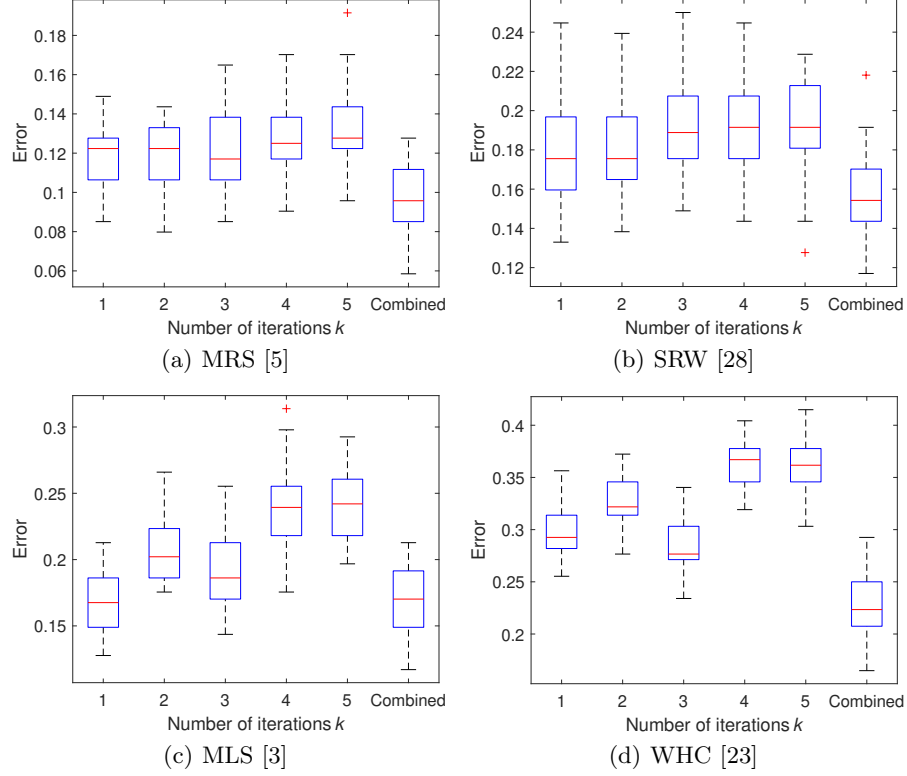
(a) MRS [5] (b) SRW [28] (c) MLS [3] (d) WHC [23]

Fig. 4. Box plots showing the confidence intervals for the detection errors for the three 3D information embedding algorithms when the number of iterations of the smoothing, k, varies during the feature extraction. The "Combined" represents the results of the combined feature set with $k \in \{1, 2, 3, 4, 5\}$ iterations.

respectively. The results when combining feature sets resulting from the application of various parameters have shown improvements in the steganalysis of the changes embedded by MRS [5], SRW [28] and WHC [23]. Meanwhile, no improvements have been observed in the case of the steganalysis on objects with the changes that have been embedded by MLS [3].

5 Conclusion

In order to improve the steganalysis results for the 3D objects, we propose to combine the 3D steganalytic feature sets obtained from 3D objects when considering various degrees of Laplacian smoothing as the input into the steganalyzers. The level of the Laplacian smoothing is controlled by two parameters: the scale factor, λ, and the number of iterations of the smoothing, k. During the experiments undertaken in this research study, we have combined the LFS76

feature sets based on the Laplacian smoothing at various levels. The steganalyzer trained over the combined feature set showed better performance than any of the individual LFS76 feature set, proposed in [14], for the steganalysis of three embedding algorithms. However, the proposed method did not improve the steganalysis results for the MLS embedding algorithm, and we believe this is due to the smoothing parameters which have not been optimally set for the embedding distortion caused by MLS. In future, we will investigate how to find the optimal smoothing parameters.

Acknowledgement

References

1. Abdulrahman, H., Chaumont, M., Montesinos, P., Magnier, B.: Color image steganalysis based on steerable gaussian filters bank. In: Proc. ACM Workshop on Information Hiding and Multimedia Security. pp. 109–114 (2016)
2. Bors, A.G., Luo, M.: Optimized 3D watermarking for minimal surface distortion. IEEE Transactions on Image Processing 22(5), 1822–1835 (2013)
3. Chao, M.W., Lin, C.h., Yu, C.W., Lee, T.Y.: A high capacity 3D steganography algorithm. IEEE Transactions on Visualization and Computer Graphics 15(2), 274–284 (2009)
4. Chen, X., Golovinskiy, A., Funkhouser, T.: A benchmark for 3D mesh segmentation. ACM Transactions on Graphics 28(3), 73:1–73:12 (2009)
5. Cho, J.W., Prost, R., Jung, H.Y.: An oblivious watermarking for 3-D polygonal meshes using distribution of vertex norms. IEEE Transactions on Signal Processing 55(1), 142–155 (2007)
6. Fridrich, J.J., Goljan, M., Hoga, D.: Steganalysis of JPEG images: Breaking the F5 algorithm. In: Proc. Workshop of Information Hiding, LNCS, vol. 2578. pp. 310–323 (2002)
7. Fridrich, J., Kodovský, J.: Rich models for steganalysis of digital images. IEEE Transactions on Information Forensics and Security 7(3), 868–882 (2012)
8. Itier, V., Puech, W.: High capacity data hiding for 3D point clouds based on static arithmetic coding. Multimedia Tools and Applications 76(24), 26421–26445 (2017)
9. Kim, D., Jang, H.U., Choi, H.Y., Son, J., Yu, I.J., Lee, H.K.: Improved 3D mesh steganalysis using homogeneous kernel map. In: Proc. Int. Conf. on Information Science and Applications. pp. 358–365 (2017)
10. Kodovsky, J., Fridrich, J.J.: Calibration revisited. In: Proc. ACM Workshop on Multimedia and Security. pp. 63–74 (2009)
11. Kodovskỳ, J., Fridrich, J., Holub, V.: Ensemble classifiers for steganalysis of digital media. IEEE Transactions on Information Forensics and Security 7(2), 432–444 (2012)
12. Li, Z., Beugnon, S., Puech, W., Bors, A.G.: Rethinking the high capacity 3D steganography: Increasing its resistance to steganalysis. In: Proc. IEEE Int. Conf. on Image Processing. pp. 510–514 (2017)

13. Li, Z., Bors, A.G.: 3D mesh steganalysis using local shape features. In: Proc. IEEE Int. Conf. on Acoustics, Speech and Signal Processing. pp. 2144–2148 (2016)
14. Li, Z., Bors, A.G.: Steganalysis of 3D objects using statistics of local feature sets. Information Sciences 415-416, 85–99 (2017)
15. Li, Z., Hu, Z., Luo, X., Lu, B.: Embedding change rate estimation based on ensemble learning. In: Proc. ACM Workshop on Information Hiding and Multimedia Security. pp. 77–84 (2013)
16. Luo, M., Bors, A.G.: Surface-preserving robust watermarking of 3-D shapes. IEEE Transactions on Image Processing 20(10), 2813–2826 (2011)
17. Ma, Y., Luo, X., Li, X., Bao, Z., Zhang, Y.: Selection of rich model steganalysis features based on decision rough set α-positive region reduction. IEEE Transactions on Circuits and Systems for Video Technology (2018), dOI: 10.1109/TCSVT.2018.2799243
18. Ren, Y., Cai, T., Tang, M., Wang, L.: AMR steganalysis based on the probability of same pulse position. IEEE Transactions on Information Forensics and Security 10(9), 1801–1811 (2015)
19. Ren, Y., Yang, J., Wang, J., Wang, L.: AMR steganalysis based on second-order difference of pitch delay. IEEE Transactions on Information Forensics and Security 12(6), 1345–1357 (2017)
20. Song, X., Liu, F., Yang, C., Luo, X., Zhang, Y.: Steganalysis of adaptive JPEG steganography using 2D gabor filters. In: Proc. ACM Workshop on Information Hiding and Multimedia Security. pp. 15–23 (2015)
21. Tang, W., Li, H., Luo, W., Huang, J.: Adaptive steganalysis based on embedding probabilities of pixels. IEEE Transactions on Information Forensics and Security 11(4), 734–745 (2016)
22. Taubin, G.: A signal processing approach to fair surface design. In: Proc. 22nd annual Conf. on Computer Graphics and Interactive Techniques. pp. 351–358 (1995)
23. Wang, K., Lavoué, G., Denis, F., Baskurt, A.: Hierarchical watermarking of semiregular meshes based on wavelet transform. IEEE Transactions on Information Forensics and Security 3(4), 620–634 (2008)
24. Wang, K., Zhao, H., Wang, H.: Video steganalysis against motion vector-based steganography by adding or subtracting one motion vector value. IEEE Transactions on Information Forensics and Security 9(5), 741–751 (2014)
25. Yang, Y., Ivrissimtzis, I.: Polygonal mesh watermarking using Laplacian coordinates. Computer Graphics Forum 29(5), 1585–1593 (2010)
26. Yang, Y., Ivrissimtzis, I.: Mesh discriminative features for 3D steganalysis. ACM Transactions on Multimedia Computing, Communications, and Applications 10(3), 27:1–27:13 (2014)
27. Yang, Y., Pintus, R., Rushmeier, H., Ivrissimtzis, I.: A steganalytic algorithm for 3D polygonal meshes. In: Proc. IEEE Int. Conf. on Image Processing. pp. 4782–4786 (2014)
28. Yang, Y., Pintus, R., Rushmeier, H., Ivrissimtzis, I.: A 3D steganalytic algorithm and steganalysis-resistant watermarking. IEEE Transactions on Visualization and Computer Graphics 23(2), 1002–1013 (Feb 2017)
29. Zhang, H., Cao, Y., Zhao, X.: A steganalytic approach to detect motion vector modification using near-perfect estimation for local optimality. IEEE Transactions on Information Forensics and Security 12(2), 465–478 (2017)
30. Zhang, Y., Qin, C., Zhang, W., Liu, F., Luo, X.: On the fault-tolerant performance for a class of robust image steganography. Signal Processing 146(2), 99–111 (2018)